ELSEVIER

Catalysis Today 28 (1996) 105–117

CATALYSIS TODAY

SMSI effect in some reducible oxides including niobia

Toshio Uchijima

Institute of Materials Science, University of Tsukuba, Tsukuba, Ibaraki 305, Japan

Abstract

Niobia is a typical SMSI oxide. High temperature reduction (HTR) exerts a reversible suppression of H_2 chemisorption on Nb_2O_5-supported or Nb_2O_5-promoted Rh or Pd catalysts. The activities of hydrogenolysis of hydrocarbons (a structure-sensitive reaction) are suppressed severely after HTR and those of hydrogenation–dehydrogenation (a structure-insensitive reaction) suffer only mild suppression. The extent of Rh–Nb_2O_5 interaction depends strongly on the preparation conditions, i.e., Nb/Rh atomic ratio, impregnation procedures and calcination temperature. A single phase $RhNbO_4$ supported on SiO_2 and similar compounds were prepared successfully, and their structural changes during HTR were studied extensively. These systems can be assumed to be a good model for SMSI. The SMSI effect was compared with several catalytic reactions which are supposed to be structure-sensitive. Usually, activities are more or less suppressed by an ensemble effect at the SMSI state, but the enhancement of catalytic activities by SMSI was found on selective hydrogenation of a carbonyl group and hydroformylation of ethylene probably by a ligand effect due to surface decoration. Recently, the role of ZnO was investigated on methanol synthesis over $Cu/ZnO/Al_2O_3$ catalysts by a combination of oxygen coverage measurements during catalysis, EDX (Energy-dispersive X-ray spectroscopy) observations and XPS studies. They gave evidence for a decoration of the Cu surface with ZnO species, leading to a formation of new active sites, tentatively expressed as Cu^+–O–Zn. The fact that SMSI does not necessarily exert only a suppression effect on catalysis will be presented as a review paper of our group.

Keywords: Niobium oxide; SMSI effect; Oxides

1. Introduction

Strong metal-support interaction (SMSI) was investigated extensively mainly on TiO_2-supported group 8 metals, leading to the model where a metal surface is covered with TiO_x species produced by a partial reduction of the support at high temperature H_2 reduction (HTR), and its recovery occurs by oxidation and subsequent low temperature reduction (LTR) [1–4]. The change between these two states takes place quite reversibly.

The model of SMSI, so-called a decoration model, was established by studies of H_2 adsorption, TPD, TPR, IR of adsorbed CO, and surface science measurements. The SMSI affects the catalytic activities in accordance with a geometric effect due to surface decoration. Catalytic activities of structure-sensitive reactions such as hydrogenolysis of hydrocarbons are strongly suppressed by SMSI, but suppression is moderate in structure-insensitive ones such as dehydrogenation of hydrocarbons [3,4].

Fig. 1 shows an extreme difference between the SMSI effect on activities of ethane hydrogenolysis and cyclohexane dehydrogenation (Fig. 1b), which compares well with the effect of metal composition of Ni–Cu alloy on the

0920-5861/96/$32.00
SSDI 0920-5861(95)00235-9

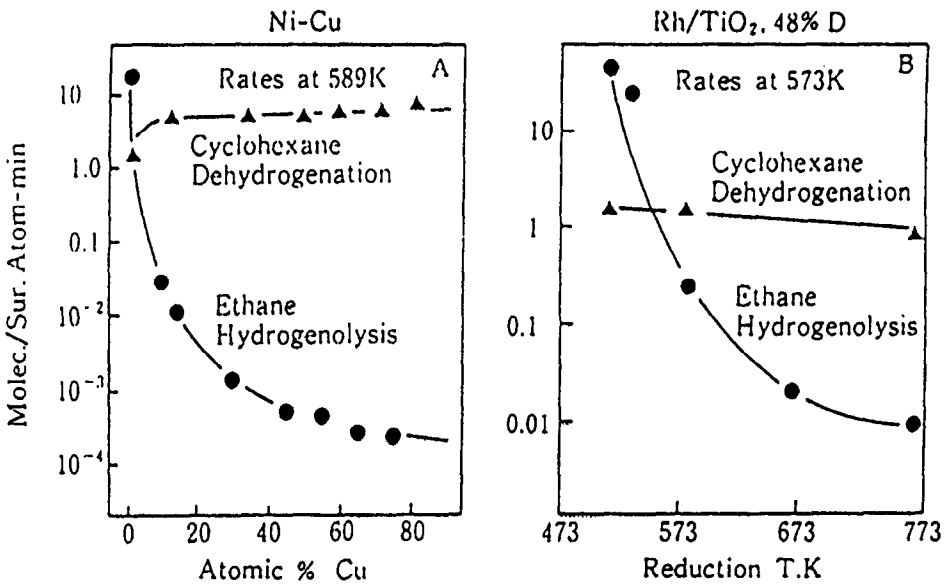

Fig. 1. Ethane hydrogenolysis and cyclohexane dehydrogenation on (a) Ni–Cu catalysts as a function of Cu content and (b) Rh/TiO_2 catalyst as a function of reduction temperature.

same catalysts (Fig. 1a) [5]. This similarity in behavior became a basis of the decoration model for SMSI.

Reportedly, SMSI occurs not only on TiO_2, but also on such reducible oxides as V_2O_3, Nb_2O_5, MnO, Al_2O_3 (containing a small amount of S: S/Pt = 0.3), La_2O_3, CeO_2, etc.

This paper will review the SMSI effect on several kinds of catalyses over niobia-supported and niobia-promoted Rh and Pd catalysts, where geometric (ensemble) effects as well as electronic (ligand) effects are shown to be important depending on the kind of catalysis.

2. SMSI on niobia-supported and niobia-promoted Rh catalysts [6–13]

The HTR effects on hydrogenolysis of hydrocarbons and CO hydrogenation were studied. Fig. 2 shows the effect of reduction temperature on the activities of Rh/Nb_2O_5 in ethane hydrogenolysis (structure-sensitive) and ethylene hydrogenation (structure-insensitive) [13]. The behavior is quite similar to Rh/TiO_2 in Fig. 1 and more drastic in the degree of suppression of hydrogenolysis activity than Rh/TiO_2 [12–14]. Almost the same relations are seen in the dehydrogenation and hydrogenolysis of cyclohexane over Rh/Nb_2O_5, as shown in Fig. 3 [15,16].

Suppression by about 2 orders of magnitude is observed in CO hydrogenation over Rh/Nb_2O_5 (Table 1) [12,16] and over niobia-promoted Rh/SiO_2 (Table 2) [17]. Although the

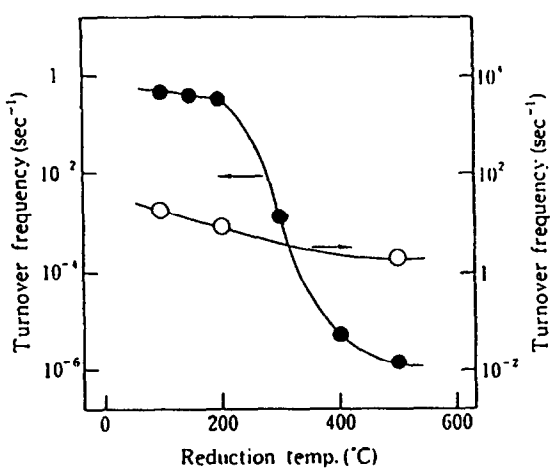

Fig. 2. Ethane hydrogenolysis and ethylene hydrogenation on 0.5 wt.-% Rh/Nb_2O_5 catalyst as a function of reduction temperature. ●: $C_2H_6 + H_2$ (162°C), ○: $C_2H_4 + H_2$ (20°C). TOF is based on the H/Rh value (0.33) after LTR at 373 K.

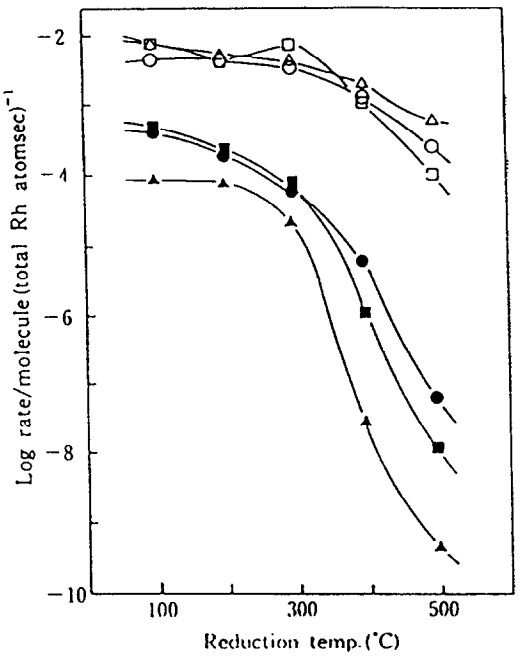

Fig. 3. The rates of the dehydrogenation and hydrogenolysis of cyclohexane over Rh/Nb_2O_5 catalysts as a function of reduction temperature. ○: 5% Rh/Nb_2O_5, □: 5% Rh/Nb_2O_5(Cl free), △: 0.5% Rh/Nb_2O_5. Open symbols: dehydrogenation, filled symbols: hydrogenolysis.

SMSI state is destroyed during CO hydrogenation probably by the role of the reaction product (H_2O) on TiO_2-supported catalysts, it is rather stable on niobia systems [14,18].

The degree of SMSI effect depends naturally on the amount of niobia addition (Nb/Rh atomic ratio), as clearly shown in Fig. 4 [10]. Rh–Nb interaction is not enough in the physical mixture of Rh/SiO_2 and Nb_2O_5. This means that the presence of both species in close contact is important for a strong interaction.

Hydrogenolysis of hydrocarbons as a typical

Table 1
Effect of the reduction temperature on the rate (10^{-4} molecule per total Rh atom per s at 473 K) of the $CO+H_2$ reaction

Catalyst	Temperature of the H_2 treatment		
	473 K (LTR)	573 K (MTR)	773 K (HTR)
0.5 wt.-% Rh/Nb_2O_5	8.8	2.6	0.18
5.0 wt.-% Rh/Nb_2O_5	1.0	0.28	0.02

Table 2
The activity of the $CO+H_2$ reaction (TOF at 500 K) and the amount of H_2 chemisorption (H/Rh) for the Nb_2O_5-promoted Rh/SiO_2 and unpromoted Rh/SiO_2 catalysts and Rh/Nb_2O_5 catalyst (0.5% Rh)

Catalyst	Nb/Rh	H/Rh		TOF (s^{-1}) [a]	
		LTR	HTR	LTR	HTR
Rh/Nb_2O_5	–	0.18	0.00	0.28	0.004
Rh/SiO_2	0	0.32	0.28	0.062	0.039
$Nb_2O_5//Rh/SiO_2$	0.9	0.16	0.11	0.39	0.15
$Nb_2O_5//Rh/SiO_2$	11.4	0.11	0.02	0.23	0.005

[a] Based on the H/Rh value after LTR at 473 K. The residence time was assumed to be defined as the ratio of the catalysts bed volume to the carrier flow rate.

structure-sensitive reaction, CO hydrogenation also as a structure-sensitive one, and dehydrogenation–hydrogenation of hydrocarbons as a typical structure-insensitive reaction were widely studied mainly on TiO_2 systems and their SMSI effects were generally accepted by the concept of ensemble effect taking a main role.

The above-mentioned behaviors in niobia systems coincide clearly with these findings: a decoration of Rh surface by partially reduced

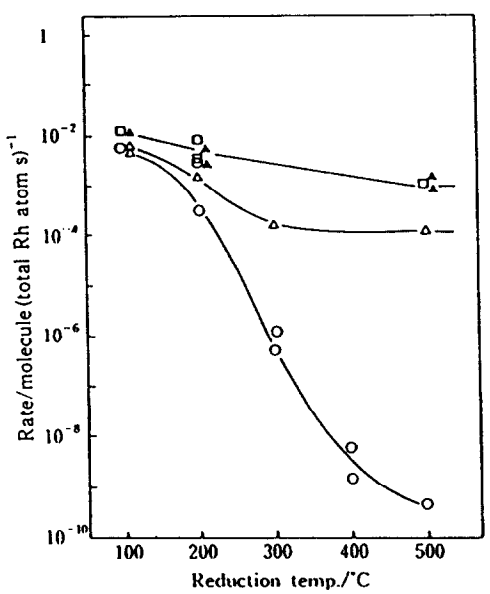

Fig. 4. Effect of catalyst reduction temperature on the rate of ethane reaction at 435 K. ○: Nb_2O_5–Rh/SiO_2, Nb/Rh = 9.3, △: Nb_2O_5–Rh/SiO_2, Nb/Rh = 0.9, □: Rh/SiO_2, ▲: Rh/SiO_2 + Nb_2O_5 (physically mixed), Nb/Rh = 9.3.

niobia species exerts an ensemble effect on these catalysts.

Fig. 5 shows the reversibility of SMSI of niobia-promoted Rh catalysts using ethane hydrogenolysis as a probe reaction [19].

As an example of another oxide than niobia, addition of even Al_2O_3 exerts SMSI effect as shown in Table 3 [20]. H/Rh and ethane hydrogenolysis are suppressed remarkably by HTR and recovered reversibly by an O_2 treatment at 400°C and subsequent LTR.

3. Strength of interaction between Rh and Nb_2O_5 and formation of new phases

The strength of interaction between Rh and Nb_2O_5 depends strongly on preparation conditions, i.e., impregnation procedure, Nb/Rh atomic ratio and calcination temperature [11,21].

Table 2 shows that the SMSI effect becomes remarkable as the Nb/Rh ratio increases at a constant calcination temperature.

The effect of impregnation procedures and calcination temperature is compared in Table 4 [11]. Catalyst C by impregnation of $RhCl_3$(aq.) on Nb_2O_5/SiO_2 and catalyst D by co-impregnation of $RhCl_3$ and $(NH_4)_3[NbO(C_2O_4)_3]$ shows only a slight interaction in terms of the extent of activity suppression of ethane hydrogenolysis after a calcination at low temperature, 400–500°C, but becomes to present an extreme SMSI effect after calcination at 700°C. That means that high temperature calcination is important for the strong Rh–Nb_2O_5 interaction.

The results of TPR are shown in Fig. 6 [11]. After O_2 treatment at 400°C, Rh/SiO_2 shows a sharp single reduction peak at 350 K (c), but it diffuses out to higher temperature on Nb_2O_5-promoted Rh catalysts [(a),(b)], which means that a hardly reducible new phase is formed by a strong Rh–Nb_2O_5 interaction.

After calcination at 1173 K, a new phase assigned to $RhNbO_4$ appears in the XRD pattern as shown in Fig. 7 [11,22]. The shift of the TPR peak to a higher temperature would be related to the formation of this new phase or its precursor by high temperature calcination. As a result, we can depict a model in Fig. 8 for the SMSI behavior in the Nb_2O_5-promoted Rh/SiO_2 catalysts [11].

By using a high temperature calcination (1173 K), almost single phase particles of $RhNbO_4$ supported on SiO_2 were prepared successfully from the systems of Nb/Rh = 1.0. The XRD spectrum is given in Fig. 9 [23]. Although there is a small contribution of Rh_2O_3, the major phase is assigned to $RhNbO_4$ [24].

Table 3
The hydrogen chemisorption and cyclohexane reaction on the promoted and unpromoted Rh/SiO_2 catalysts

Catalyst	Treatment [a]	H/Rh [b]	Rate [c] at 500 K cyclohexane	
			Dehydrogenation [d]	Hydrogenolysis [e]
Rh/SiO_2	LTR	0.34	0.018	0.80×10^{-3}
	HTR	0.28	0.045	1.26×10^{-3}
$Al_2O_3//Rh/SiO_2$	LTR	0.23	0.108	8.74×10^{-3}
	HTR	0.06	0.108	0.48×10^{-3}
Rh/Al_2O_3	LTR	0.98	0.104	1.25×10^{-2}
	HTR	0.94	0.131	1.94×10^{-2}

[a] LTR and HTR imply low-temperature reduction at 473 K and high-temperature reduction at 773 K, respectively, preceded by O_2 treatment at 673 K.
[b] Atomic ratio of chemisorbed H to total Rh.
[c] Molecules converted per total Rh atoms per s.
[d] Rate of benzene formation.
[e] The main product was CH_4.

Table 4
The extent of Rh–Nb_2O_5 interaction in Nb_2O_5-promoted Rh/SiO_2 catalysts (0.5 wt.-% Rh)

Catalyst [a]	Nb/Rh	Impregnation procedure	Calcination temperature (°C)	Extent of activity suppression [b]
A [c]	9.3	$(NH_4)_3[NbO(C_2O_4)_3]$ (aq.) on SiO_2	500	$10^{-7.0}$
B	9.3	$NbCl_5$/ethanol on Rh/SiO_2	500	$10^{-2.0}$
C	9.3	$RhCl_3$(aq) on Nb_2O_5/SiO_2 [d]	500	$10^{-1.5}$
			700	$10^{-4.0}$
D	1.0	Co-impregnation of $RhCl_3$ (aq.) and $(NH_4)_3$ $[NbO(C_2O_4)_3]$	400	$10^{-1.0}$
			700	$10^{-5.5}$

[a] The SiO_2 support used here was the JRC-SIO-3.
[b] The ratio of the catalytic activity for ethane hydrogenolysis after the HTR at 500°C with that after the O_2 treatment at 400°C followed by LTR at 100°C (r(HTR)/r(LTR)).
[c] The same catalyst as in Section 3.1.
[d] The promoted support (Nb_2O_5/SiO_2) was calcined at 700°C for 3 h before impregnation of $RhCl_3$(aq.).

Other new mixed oxide particles supported on SiO_2, i.e., $RhVO_4$, $MnRh_2O_4$ and $MoRh_2O_6$, were prepared by similar procedures [25]. Their properties such as crystal structure, particle size and decomposition temperature in H_2 are summarized in Table 5.

Structural changes of $RhNbO_4$ and $RhVO_4$ in H_2 were extensively studied by TPR, TPO, TPD of H_2 and XRD. The results enable us to propose the model for the structural changes of these supported mixed oxides as shown in Fig. 10 [22,23]. Either $RhNbO_4$ or $RhVO_4$ decomposes into finely dispersed Rh metal in H_2 at 773 K, the surface of which is covered with NbO_2 or V_2O_3, respectively, produced by reductive decomposition of the double oxides. We can visualize SMSI phenomena by these structural changes of $RhNbO_4$ and $RhVO_4$.

The $RhNbO_4/SiO_2$ catalyst shows a typical SMSI behavior in the catalytic activity of ethane

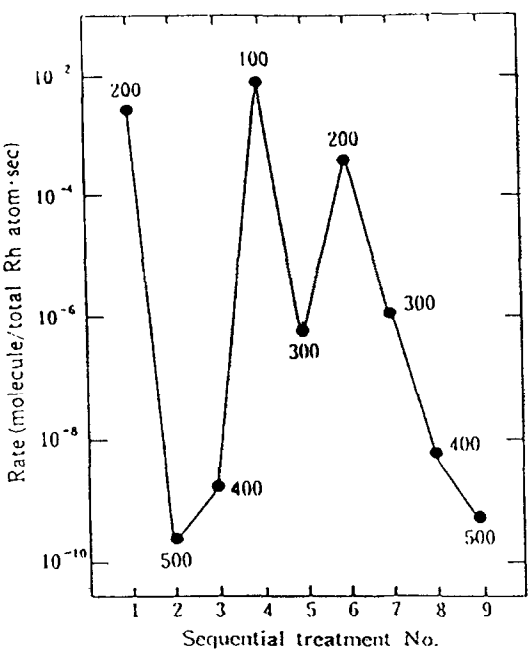

Fig. 5. The change in the ethane hydrogenolysis activity of the Nb_2O_5-promoted Rh/SiO_2 catalyst (Nb/Rh = 9.3) after the sequential O_2 treatment at 673 K followed by the H_2 reduction at different temperatures indicated in the figure.

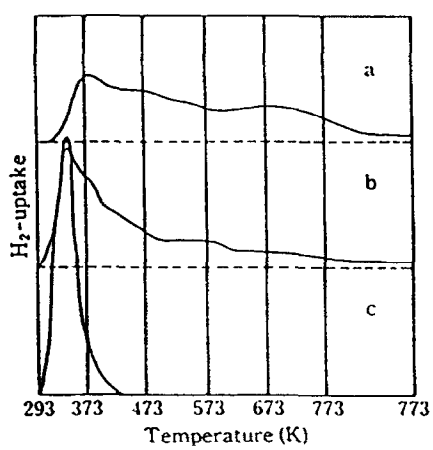

Fig. 6. TPR spectra of Nb_2O_5-promoted 0.5% Rh/SiO_2 catalysts: (a) Nb/Rh = 9.3, (b) Nb/Rh = 0.9 and (c) Nb/Rh = 0. The O_2 treatment at 400°C was performed before the TPR run, where catalyst temperature was ramped at 5 K/min.

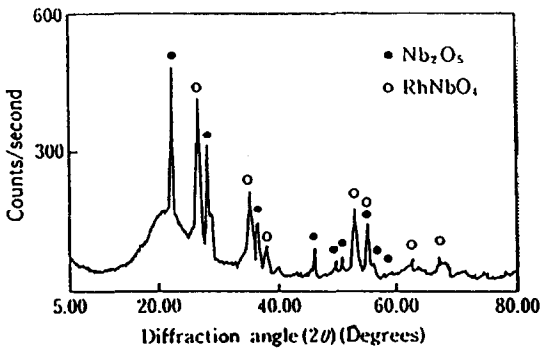

Fig. 7. X-Ray diffraction pattern of the Nb_2O_5-promoted 5.0 wt.-% Rh/SiO_2 catalyst (Nb/Rh = 3.1) after being calcined in air at 1173 K.

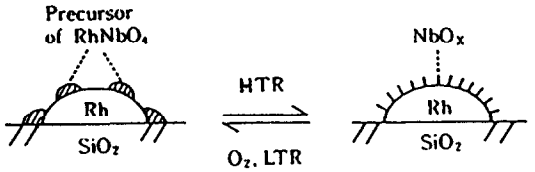

Fig. 8. A model for the SMSI behavior in the Nb_2O_5-promoted Rh/SiO_2 catalysts.

hydrogenolysis [23]. The activity is rather low after it is decomposed by a first HTR treatment (Fig. 11, No. 1), but increases remarkably by O_2 treatment at 400°C and subsequent LTR at 100 and 200°C (Nos. 3 and 2, respectively). The activity is strongly suppressed again by repeating HTR (No. 4).

The extent of metal–oxide interaction of all the Rh double oxides is summarized in Table 6, using ethane hydrogenolysis as a probe reaction [25]. All the Rh double oxides show the SMSI behavior, but its extent differs among them.

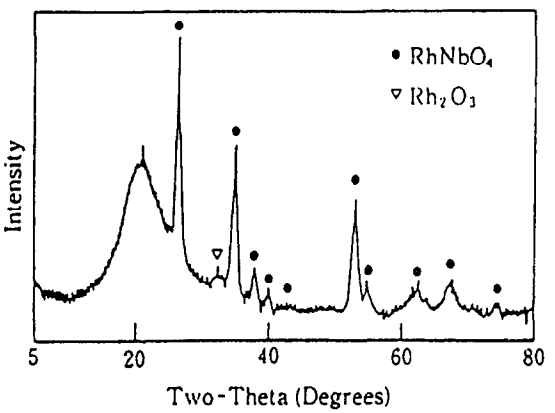

Fig. 9. X-Ray diffraction pattern of the Nb_2O_5-promoted 4.0 wt.-% Rh/SiO_2 catalyst (Nb/Rh = 1) after being calcined at 1173 K.

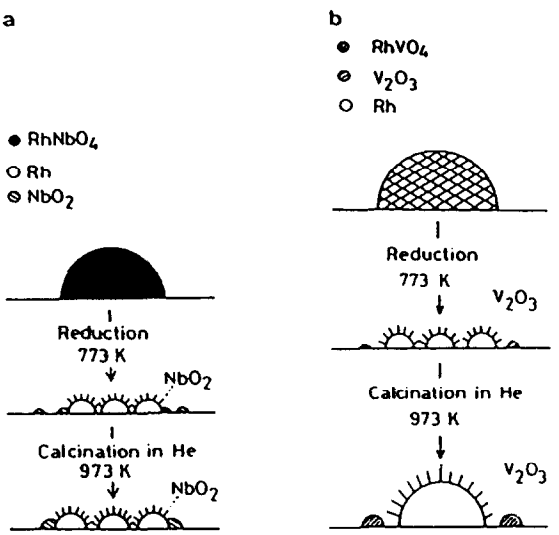

Fig. 10. A model for the behaviors of promoted Rh/SiO_2 catalysts during the treatment in H_2 and He at high temperature. (a) Niobia-promoted Rh/SiO_2 catalyst, (b) vanadia-promoted Rh/SiO_2 catalyst.

Table 5
Formation of the mixed oxides on SiO_2 surface by the calcination treatment

Mixed oxide	Calcination temp. (°C)	Crystal structure	Particle size (Å)	Decomposition temp. in H_2 (°C)
$RhNbO_4$	700–900	rutile type	140	300
$RhVO_4$	500–700	rutile type	190	200
$MnRh_2O_4$	900	spinel type	> 300	300
$MoRh_2O_6$	700	rutile type	140	200

4. Does SMSI always exert suppression in catalytic activities? [26–28]

The changes of catalytic activities by HTR are compared with several catalytic activities, which are supposed to be more or less structure-sensitive.

4.1. H_2 chemisorption

Fig. 12 shows the effect of reduction temperature on the adsorption capacity of H_2 of Rh/Nb_2O_5 and Pd/Nb_2O_5. These two catalysts show typical SMSI behaviors, although the extent of suppression and curve shapes are slightly different.

4.2. Cyclohexane reaction

Fig. 13 shows the Arrhenius plots of catalytic activities of cyclohexane dehydrogenation on Rh/Nb_2O_5 after H_2 treatment at different temperatures. After HTR at 400 to 500°C, activities

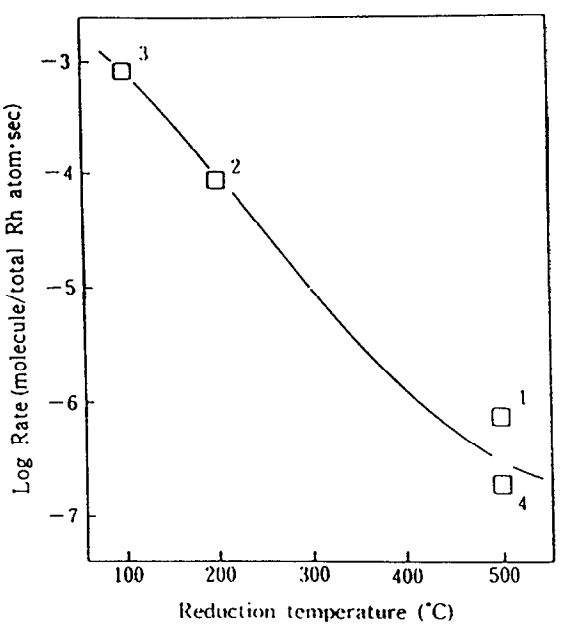

Fig. 11. Effect of reduction temperature on the ethane hydrogenolysis activity (162°C) after the $RhNbO_4/SiO_2$ catalyst was decomposed in H_2. The O_2 treatment at 400°C was performed before the H_2 reduction at the given temperature.

Table 6
The extent of metal-oxide interaction after the Rh double oxides were decomposed on SiO_2 by HTR at 500°C (Rh content: 5 wt.-%)

Metal-oxide	Rh particle size (Å) [a]	Extent of activity suppression [b]
Rh only [c]	140	$10^{-0.4}$
Rh–Nb [d]	< 30	$10^{-5.5}$
Rh–Nb	48	$10^{-3.5}$
Rh–V	43	$10^{-3.5}$
Rh–Mn	120	$10^{-3.0}$
Rh–Mo	145 [e]	$10^{-2.0}$

[a] After HTR at 500°C.
[b] r(HTR)/r(LTR) (see Table 5).
[c] Rh/SiO_2 calcined at 900°C.
[d] 0.5 wt.-% Rh.
[e] Formation of $MoRh_3$.

are suppressed to 10^{-1}–10^{-2} in parallel to the suppression of H/Rh, although the dependence with H/Rh is not completely parallel in the region of low-temperature treatments. In this structure-insensitive reaction, an other effect than a simple geometric one seems to be effective.

The effect of reduction temperature on hydrogenolysis of cyclohexane is compared between Rh/Nb_2O_5 and Rh/Al_2O_3 in Fig. 14. The activities of dehydrogenation are also plot-

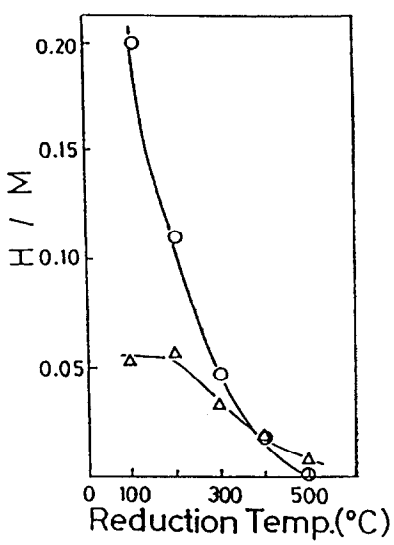

Fig. 12. Effect of reduction temperature on the adsorption capacity of H_2. ○: 0.5% Rh/Nb_2O_5, △: 5% Pd/Nb_2O_5.

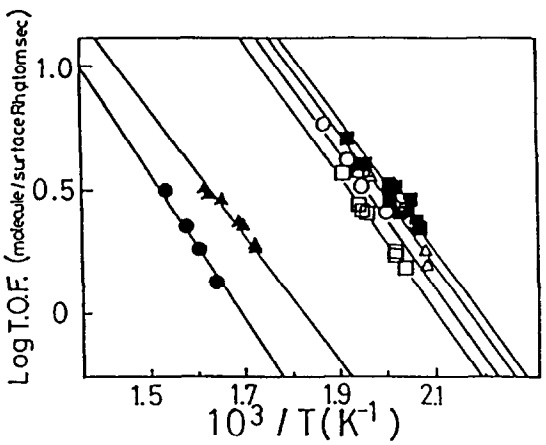

Fig. 13. Arrhenius plots of catalytic activities of cyclohexane dehydrogenation on 0.5% Rh/Nb_2O_5 after H_2 treatment at different temperatures. ■: H_2, 100°C, △: H_2, 200°C, ○: H_2, 300°C, □: H_2, 400°C, ▲: H_2, 450°C, ●: H_2, 500°C. $H_2/C_6H_{12} = 0$.

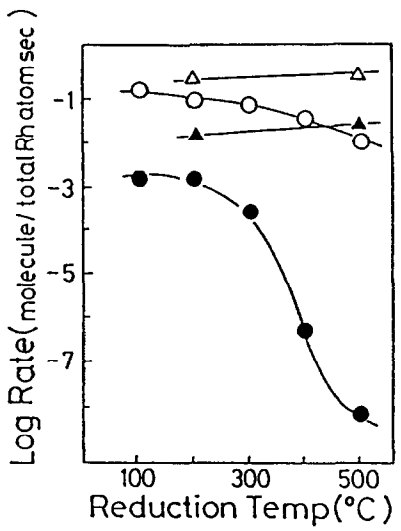

Fig. 14. Effect of reduction temperature on the activities of dehydrogenation and hydrogenolysis of cyclohexane over 0.5% Rh/Nb_2O_5 and 0.5% Rh/Al_2O_3. Dehydrogenation ○: 0.5% Rh/Nb_2O_5, △: 0.5% Rh/Al_2O_3. Hydrogenolysis ●: 0.5% Rh/Nb_2O_5, ▲: 0.5% Rh/Al_2O_3. $H_2/C_6H_{12} = 40$. Reaction temperature: 162°C.

ted. The activity of hydrogenolysis is suppressed to 10^{-5}–10^{-6} after HTR on Rh/Nb_2O_5, but no suppression is observed on Rh/Al_2O_3.

This phenomenon can be used for a selectivity control by HTR in the cyclohexane reaction over Rh/Nb_2O_5: only the hydrogenolysis can be diminished selectively to a negligible level. It is not possible over Rh/Al_2O_3.

4.3. Decomposition of ammonia

The activities of ammonia decomposition and its activation energies are compared with Rh/SiO_2, Nb_2O_5-promoted Rh/SiO_2 and Rh/Nb_2O_5 catalysts as a function of reduction

Table 7
Effect of reduction temperature of Rh catalysts on activities of ammonia decomposition and its activation energies

Catalyst	Red. temp (°C)	H/Rh	Log Rate [a,b]	E [c] (kcal/mol)
0.5% Rh/SiO_2	200	0.32	1.79	35.7
	500	0.28	1.73	35.7
Nb_2O_5–Rh/SiO_2 (Nb/Rh = 11.4)	200	0.07	0.18	28.8
	300	0.043	0.62	28.4
	400	0.03	0.75	29.7
	500	0.02	0.29	27.5
Nb_2O_5–Rh/SiO_2 (Nb/Rh = 0.9)	200	0.16	1.93	24.7
	500	0.10	1.93	25.2
0.5% Rh/Nb_2O_5	200	0.11	0.81	24.3
	300	0.046	0.67	23.8
	400	0.018	0.27	23.8
	500	0.00	0.21	24.7

[a] Reaction temperature: 460°C.
[b] Molecules converted per total Rh atoms per s.
[c] Activation energy.

temperature in Table 7. Although it is difficult to get obvious tendencies, addition of Nb_2O_5 promotes the catalysis in a circumstance of Nb/Rh = 0.9 after LTR, and the activities increase a little, do not change much or decrease slightly after HTR in many cases with Nb_2O_5-promoted or Nb_2O_5-supported systems.

Ammonia decomposition is usually treated as a structure-sensitive reaction. So, we can anticipate that the activity would suffer a severe suppression due to the ensemble effect by a decoration of the Rh surface with NbO_2 after HTR, but the results suggest otherwise. Action of some electronic or ligand effects would be important in this catalysis.

In Fig. 15, the specific activities are replotted as a function of reduction temperature, where the values are based on the H_2 adsorption after reduction treatments at each temperature.

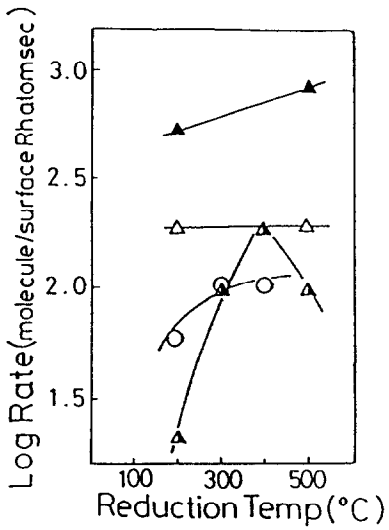

Fig. 15. Effect of reduction temperature on the activities of ammonia decomposition over Rh/Nb_2O_5 and Rh/SiO_2. ○: Rh/Nb_2O_5, △: Rh/SiO_2, ▲: Nb_2O_5-promoted Rh/SiO_2 (Nb/Rh = 0.9), half-filled triangle :Nb_2O_5-promoted Rh/SiO_2 (Nb/Rh = 11.4). Reaction temperature: 460°C.

4.4. CO hydrogenation

Over Rh/Nb_2O_5 and highly loaded Nb_2O_5–Rh/SiO_2 (Nb/Rh = 11.4) catalysts, activities of CO hydrogenation are suppressed by two orders of magnitude after HTR, but change little over Rh/SiO_2 and Nb_2O_5–Rh/SiO_2 of a low loading (Nb/Rh = 0.9) as shown in Fig. 16.

As an interesting observation, activities after LTR are obviously enhanced over Nb_2O_5-supported and Nb_2O_5-promoted catalysts as compared to Rh/SiO_2. As shown in Table 8, activation energies are clearly lowered by using Nb_2O_5 as support or promoter. In addition to a suppression due to an ensemble effect by decoration of the Rh surface, Nb_2O_5 or NbO_2 acts as a promoter of this catalysis probably through a change of the electronic state of Rh by a ligand effect.

IR studies of adsorbed CO show the shift of linear CO absorption by the decoration of Rh surface, suggesting the change of electronic state of Rh. Attached NbO_2 is considered to promote the dissociation of adsorbed CO.

Table 8
Effect of reduction temperature of Rh catalysts on CO hydrogenation activities and adsorption capacities of hydrogen

Catalyst	H/Rh		T.O.F. [a,b,c]		E (kcal/mol)	
	200 [d]	500 [d]	200 [d]	500 [d]	200 [d]	500 [d]
0.5% Rh/SiO_2	0.32	0.28	1.2	0.78	25.1	26.5
Nb_2O_5–Rh/SiO_2 (Nb/Rh = 0.88)	0.16	0.10	7.8	3.0 (5.0 [e])	18.3	17.8
Nb_2O_5–Rh/SiO_2 (Nb/Rh = 11.4)	0.11	0.02	4.6	0.092 (0.5 [e])	18.3	17.8
0.5% Rh/Nb_2O_5	0.18	0.00	5.6	0.088	17.4	17.4
5% Rh/Nb_2O_5	0.047	0.00	64.0	0.3	18.3	16.9

[a] Molecules converted per surface Rh atoms per s.
[b] Reaction temperature: 227°C.
[c] Based on H/Rh values after LTR treatment.
[d] Reduction treatment temperature (°C).
[e] Based on H/Rh value after HTR treatment.

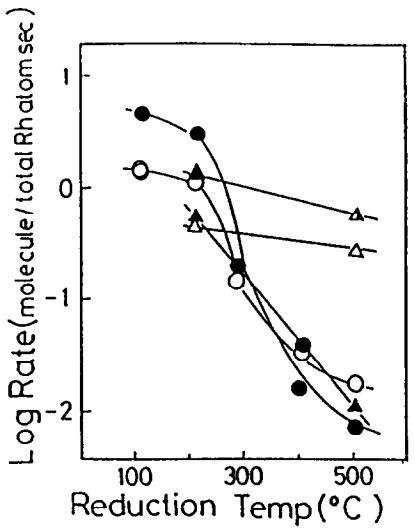

Fig. 16. Effect of reduction temperature on the activities of CO hydrogenation over Rh/Nb_2O_5, Nb_2O_5-promoted Rh/SiO_2 and Rh/SiO_2 catalysts. ○: 0.5% Rh/Nb_2O_5, ●: 5% Rh/Nb_2O_5, △: 0.5% Rh/SiO_2, half-filled triangle: Nb_2O_5-promoted Rh/SiO_2 (Nb/Rh = 0.9), ▲: Nb_2O_5-promoted Rh/SiO_2 (Nb/Rh = 11.4). Reaction temperature: 227°C.

4.5. Hydrogenation of carbonyl compounds

Table 9 shows the HTR effect on catalytic activities of acetone hydrogenation over Rh/Nb_2O_5. The formation of isopropyl alcohol is suppressed by about one order of magnitude after HTR, whereas propane, as a deep hydrogenation product, becomes undetectable. Similarly, in the hydrogenation of butyl aldehyde over Rh/Nb_2O_5, the activity of butyl alcohol formation is suppressed by 1.5 orders of magnitude after HTR and that of hydrogenolysis becomes zero, as shown in Table 10.

The results of Pd/Nb_2O_5 are shown in Table 11. Propane disappears completely, similar to Rh/Nb_2O_5 after HTR, whereas the formation of isopropyl alcohol is enhanced by about two times, which is in contrast to the result of Rh/Nb_2O_5.

This is an example where SMSI promotes catalysis on occasion. Deep hydrogenation and hydrogenolysis are severely suppressed by the ensemble effect due to surface decoration, but attached NbO_2 is supposed to exert the ligand effect in favor of the selective hydrogenation of the carbonyl group.

Table 9
Catalytic activities of acetone hydrogenation over Rh/Nb_2O_5

Red. temp. (°C)	Rate [a]			E_a (kcal/mol)	
	Total	i-C_3H_7OH	Propane	i-C_3H_7OH	Propane
200	0.28	0.20	0.08	13.7	20.6
500	0.03	0.03	– [b]	13.7	– [b]

[a] Molecules converted per total Rh atoms per s, at 180°C.
[b] Not detected.

Table 10
Hydrogenation activities of butyraldehyde over Rh/Nb_2O_5 catalyst (TOF at 72°C) [a]

Red. temp (°C)	Total	n-C_4H_9OH	Hydrogenolysis
200	4.7	3.6	1.1
500	0.2	0.2	– [b]

[a] Molecules converted per surface Rh atoms per s.
[b] Not detected.

Table 11
Hydrogenation activities of acetone over Pd/Nb_2O_5 catalyst (rate at 175°C)

Red. Temp. (°C)	Rate [a]			E_a (kcal/mol)	
	Total	i-C_3H_7OH	Propane	i-C_3H_7OH	Propane
200	0.106	0.041	0.065	22.9	22.8
500	0.085	0.085	– [b]	13.7	– [b]

[a] Molecules converted per total Rh atoms per s.
[b] Not detected.

4.6. Hydroformylation of ethylene

The results of hydroformylation of ethylene over Pd/Nb_2O_5 are shown in Table 12. The products are ethane by hydrogenation of ethy-

Table 12
Effect of reduction temperature of 5% Pd/Nb_2O_5 catalyst on hydroformylation of ethylene

Red. temp. (°C)	Yield [b] ($\times 10^{-3}$ molec./surf. Pd s)			E_a (kcal/mol)	
	C_2H_6	Oxo product	Total	C_2H_6	Oxo product
200	5.78	0.00	5.78	13.7	–
500	3.74	4.77	8.51	12.8	12.8

[a] Reaction temperature: 60°C.
[b] Based on H/Pd value after LTR treatment.

Table 13
Effect of reduction temperature of 5% Pd/TiO_2 catalyst on hydroformylation of ethylene

Red. temp. (°C)	Yield [b] ($\times 10^{-3}$ molec./surf. Pd s)			E_a (kcal/mol)	
	C_2H_6	Oxo product	Total	C_2H_6	Oxo product
200	0.62	0.26	0.88	13.3	17.4
500	0.52	1.62	2.14	12.8	13.7

[a] Reaction temperature: 20°C.
[b] Based on H/Pd value after LTR treatment.

lene and oxo products by insertion of CO to ethylene. The main component of the oxo products was 2-methyl-2-pentenal formed by dehydro-condensation of propionaldehyde.

Total activities increase slightly after HTR. Remarkable points are that oxo products become a main product after HTR but are not formed after LTR. The formation of ethane is suppressed only slightly after HTR.

Similar results were obtained over Pd/TiO_2 as shown in Table 13. The formation of oxo product is greatly enhanced and that of ethane is suppressed slightly.

Fig. 17 shows the change of IR spectra of adsorbed CO on Pd/TiO_2 as a function of reduction temperature. Two kinds of bridged CO at 1995 and 1938 cm^{-1} appear after LTR, but they decrease as the reduction temperature is increased, where in turn a new peak due to linear CO at 2090 cm^{-1} grows by reduction at 400°C. As the metal surface is blocked with NbO_2 species, sites of two adjacent metals necessary for bridged CO adsorption are diminished and then bridged CO species change into linear ones which are surrounded with NbO_2 on the metal surface.

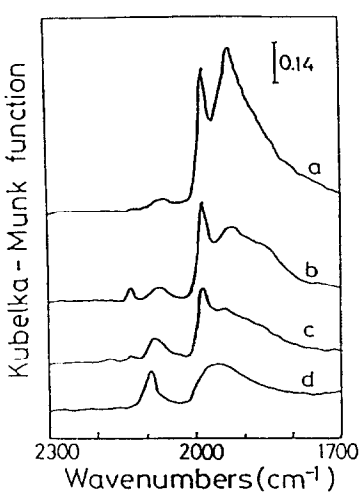

Fig. 17. Effect of reduction temperature on IR spectra of adsorbed CO on Pd/TiO_2. (a) H_2, 100°C, (b) H_2, 200°C, (c) H_2, 300°C and (d) H_2, 400°C.

We speculate that this linear CO species adjacent to NbO_2 is responsible for the enhancement of oxo product formation by a suppression of CO dissociation and an acceleration of CO insertion as a result of the ligand effect by NbO_2.

The SMSI effect was studied on seven kinds of catalytic reactions. SMSI leads usually to more or less suppression of catalytic activities by an ensemble effect, but in some cases it exerts an enhancement of activities by a ligand effect. These results are summarized in an approximate way in Tables 14 and 15.

5. Methanol synthesis over $Cu/ZnO/Al_2O_3$ [29–33]

The active center for this catalyst in methanol synthesis and the role of ZnO as an accelerator

Table 14
Comparison of activity changes and activation energies of several catalysts between LTR and HTR over 0.5% Rh/Nb_2O_5 catalyst

Reaction	Activity change [a]	E (kcal/mol)	
		LTR [b]	HTR [c]
H/M	−1	–	–
Ethane hydrogenolysis	−6 to −7	34.7	33.3
Cyclohexane dehydrogenation	−1	10.5	11.0
Cyclohexane hydrogenolysis	−5 to −6	26.1	27.5
Ammonia decomposition	−0.6	24.3	24.7
CO hydrogenation	−2	17.4	17.4
Butyraldehyde hydrogenation	−1	12.8	12.8
Acetone hydrogenation	−1	13.7	13.7

[a] Log[Rate(HTR)/Rate(LTR)].
[b] Reduction temperature: 200°C.
[c] Reduction temperature: 500°C.

Table 15
Comparison of activity changes and activation energies of several catalysts between LTR and HTR over 5% Pd/Nb_2O_5 catalyst

Reaction	Activity change [a]	E (kcal/mol)	
		LTR [b]	HTR [c]
H/M	−1	–	–
Acetone hydrogenation	0.3	22.9	13.7
Ethylene hydrogenation	−0.1	13.7	12.8
Ethylene hydroformylation	∞ [d]	– [d]	12.8

[a] log[Rate(HTR)/Rate(LTR)].
[b] Reduction temperature: 200°C.
[c] Reduction temperature: 500°C.
[d] No oxo product detected after LTR.

have been a matter of controversy for long years.

We have recently studied this subject and clarified the role of ZnO, the main results of which will be briefly introduced here.

Specific activities of methanol synthesis were compared among many Cu/metal oxides and Cu/ZnO/metal oxides. The activities can be expressed by a single relation of mountain shape

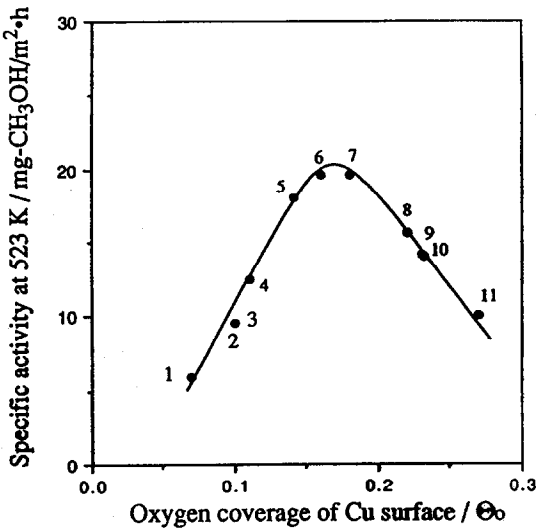

Fig. 18. Specific activity at 523 K as a function of oxygen coverage of Cu surface. Reaction conditions: $H_2/CO_2 = 3$, Feed gas rate = 300 cm^3/min, Total pressure = 5.0 MPa, Catalyst weight = 1.0 g. Catalysts composition (wt.-%): 1. Cu/SiO_2 (30/70), 2. Cu/Al_2O_3 (50/50), 3. Cu/ZrO_2 (50/50), 4. Cu/Cr_2O_3 (50/50), 5. $Cu/ZnO/Cr_2O_3$ (50/40/10), 6. $Cu/ZnO/Ga_2O_3$ (50/25/25), 7. Cu/Ga_2O_3 (50/50), 8. $Cu/ZnO/Al_2O_3$ (50/45/5), 9. Cu/ZnO (50/50),10. $Cu/ZnO/ZrO_2$ (50/25/25). 11. $Cu/ZnO/La_2O_3$ (50/40/10).

as a function of oxygen coverage of Cu, which was measured by N_2O adsorption after reaction, where its maximum is at an oxygen coverage of about 0.16 (Fig. 18). This result suggests the covering of Cu surface by ZnO species during the catalysis.

Then, physical mixtures of Cu/SiO_2 and ZnO/SiO_2 powders were studied. Both catalytic activities and oxygen coverage increase in parallel as a function of reduction temperature as pretreatment. EDM observations gave evidence of ZnO migration onto Cu surface. On ZnO/SiO_2 powders, only a peak due to Zn exists irrespective of reduction temperature, but a peak of Zn grows on Cu/SiO_2 powders as the reduction temperature is increased.

Zn is supposed to migrate onto the Cu surface through the gas phase, and to be oxidized to ZnO during catalysis, which gives an enhancement effect.

XPS studies on model catalysts of Cu crystal with deposited Zn gave evidence to support the above model: the attached ZnO gives an acceleration effect on the catalysis. We tentatively propose the formation of such a new active site as Cu^+–O–Zn.

The above picture is very similar to SMSI as a sense of surface decoration. So, this is another example, in which, surface decoration creates new active sites and accelerates catalysis.

Acknowledgements

The present studies were collaborated with Dr. K. Kunimori, Dr. J. Nakamura and Dr. T. Fujitani.

References

[1] S.J. Tauster et al., J. Am. Chem. Soc., 100 (1978) 170.
[2] S.J. Tauster et al., Science, 211 (1981) 1121.
[3] S.A. Stevenson et al. (Editors), Metal-Support Interactions in Catalysis, Sintering and Redispersion, Van Nostrand-Reinhold, New York, 1987.
[4] G.L. Haller and D.E. Resasco, Adv. Catal., 36 (1989) 173.

[5] D.E. Resasco and G.L. Haller, J. Catal., 82 (1983) 279.
[6] A.K. Singh et al., J. Catal., 94 (1985) 422.
[7] E.I. Ko et al., J. Catal., 95 (1985) 260.
[8] G.B. Mcviker and J.J. Ziemiak, J. Catal., 95 (1985) 473.
[9] Y.-J. Lin et al., J. Chem. Soc., Faraday Trans. 1, 83 (1987) 2091.
[10] K. Kunimori et al., J. Chem. Soc., Chem. Commun., (1986) 966.
[11] Z. Hu et al., J. Catal., 112 (1988) 478.
[12] K. Kunimori et al., Chem. Lett., (1983) 1619.
[13] K. Kunimori et al., Chem. Lett., (1986) 573.
[14] K. Kunimori et al., Proc. 8th Int. Congr. Catal., V (1984) 251.
[15] D.E. Resasco and G.L. Haller, Stud. Surf. Sci. Catal., 11 (1982) 105.
[16] K. Kunimori et al., Proc. 8th Japan-USSR Seminar, (1986) 115.
[17] T. Uchijima and K. Kunimori, Report of Special Project Research on Energy under Grant in Aid of Scientific Research of the Ministry of Education, Science and Culture, Japan (SPEY 16), 1987, p. 233.
[18] K. Kunimori et al., Chem. Lett., (1985) 359.
[19] K. Kunimori et al., Shokubai, 29 (1987) 106.
[20] Z. Hu et al., Chem. Lett., (1986) 2079.
[21] K. Kunimori et al., Proc. 2nd Int. Conf. Spillover, (1989) 96; Appl. Catal., 53 (1989) L11; Catal. Today, 8 (1990) 85; Catal. Lett., 7 (1990) 337; ibid., 9 (1991) 331; 10th Int. Congr. Catal., (1992).
[22] Z. Hu et al., J. Catal., 119 (1989) 33; ibid., 127 (1991) 276.
[23] Z. Hu et al., Catal. Lett., 1 (1988) 271.
[24] I.S. Shaprygin et al., Russ. J. Inorg. Chem., 23 (1978) 773.
[25] K. Kunimori et al., Shokubai, 31 (1989) 60.
[26] A. Maeda et al., Catal. Lett., 1 (1988) 155.
[27] A. Maeda et al., Nippon Kagaku Kaishi, 3 (1992) 267.
[28] A. Maeda et al., Catal. Lett., 4 (1990) 107.
[29] T. Fujitani et al., Catal. Lett., 25 (1994) 271.
[30] Y. Kanai et al., Catal. Lett., 27 (1994) 67.
[31] T. Fujitani et al., Chem. Lett., (1994) 1887.
[32] T. Fujitani et al., Appl. Catal. A, 125 (1995) L119.
[33] J. Nakamura et al., Catal. Lett., 31 (1995) 325.